ELSEVIER

Catena 49 (2002) 171–181

CATENA

www.elsevier.com/locate/catena

Effect of composition and physical properties of natural kaolinitic clays on their strong acid weathering rates

David Hradil*, Jiří Hostomský

Institute of Inorganic Chemistry, Academy of Sciences of the Czech Republic, 250 68 Řež, Czech Republic

Received 10 July 2000; accepted 21 February 2001

Abstract

Two samples of pure kaolinite with a significant difference in their crystallinity, a commercial kaolin sample with 20 wt.% of illitic component and one sample of illitic clay with up to 20 wt.% of kaolinitic component were used in dissolution kinetic experiments and the results compared to data obtained from the leaching of sandstone matrix kaolinites under laboratory conditions. The mineralogical and chemical compositions of all samples were characterised using X-ray diffraction and X-ray fluorescence techniques. Specific surface area was measured by the gas adsorption (BET) method. Structural disorder of kaolinite given by the extent of the sheet translations was calculated from the X-ray diffraction data (the 'Hinckley index'). Dissolution experiments in continuously stirred suspensions (with solid/liquid ratio=1:100) were performed in 0.5 and 5 M solutions of H_2SO_4 at 25 and 40 °C, respectively, and the reaction rate was calculated from the measured concentrations of Al and Si in the solution. It was found that slight non-stoichiometry in the steady state stage of dissolution with preferential removal of aluminium is a common feature. It can be augmented by the presence of impurities, such as aluminium phosphates (crandallites). Acid weathering rates increase with structural disorder of kaolinite but observed differences cannot be fully explained by the diversity of crystal lattice structures. The contribution of illite to the dissolution process is very small; and thus, illitic admixtures cause the deceleration of the acid decomposition of natural kaolinitic clays. When calculating solute transport in acidified profiles it is suggested that the changes of the kinetic parameters of kaolinite due to the presence of poorly ordered structures (increasing the rate) and to the presence of 2:1 structures (such as illites, decreasing the rate) in mineral assemblages should be taken into consideration. © 2002 Elsevier Science B.V. All rights reserved.

Keywords: Kaolinite; Illite; Dissolution; Weathering rate; Sulphuric acid

---

* Corresponding author. Tel.: +420-2-66172187; fax: +420-2-20941502.
E-mail address: hradil@iic.cas.cz (D. Hradil).

PII: S0341-8162(02)00024-3

1. Introduction

The presence of inorganic acids in weathering crusts and soils has certainly been underestimated. Their formation is mainly due to oxidation mechanisms. For instance, H_2SO_4 can be formed by oxidation of sulphur compounds (S, H_2S, FeS_2) present in the rock itself or in acid rain. These acid solutions are thought to cause the destruction of clays; under low pH conditions, aluminium and other major cations are more soluble than silicon that can precipitate as opal in voids and channels of the sediment and form silcretes. Thiry et al. (1988) found that weathering cover and the Tertiary deposits in the southern Paris basin are affected by intense silica leaching (indicated by the dissolution of clay minerals and the corrosion of detrital quartz grains) in the upper levels of the Fontainebleau Sand. This leaching has to be related to strong acid conditions resulting from oxidation of the primary minerals (Thiry and Simon-Coinçon, 1996). The form of the matrix of Australian groundwater silcretes and conservation of primary sedimentary structures and fabrics suggest undoubtedly in situ destruction of sedimentary clays under acid conditions at the water table and the subsequent production of secondary silica phases (Milnes and Thiry, 1992).

At present, dilute solutions of sulphuric acid are produced mainly because of human activities such as mining (acid mine waters) and combustion of fossil fuels (acid rain). Aluminium released from decomposed octahedral structures of clay minerals can increase the toxicity and salinity of ground and surface waters in polluted areas. For example, water coming from a pyrite-rich waste dump of the Šobov quartzite deposit in Slovakia is enriched by Al (1.5 g/l), Fe (3.6 g/l) and SO_4^{2-} (16.5 g/l) and its pH varies between 1.5 and 2.3. Aluminium is released mostly from pyrophyllite and illite that prevail in the surrounding rocks (Šucha et al., 1994). In the Stráž pod Ralskem uranium deposit (Northern Bohemia), the in-situ leaching method has been used since the year 1968 and more than 4 million tons of H_2SO_4 have been injected to the Cenomanian aquifer in quartz sandstones. Kaolinite in the sedimentary matrix is the major reactant with these acidic solutions and a major source of aluminium in ground waters, where Al concentrations varied between 4 and 6 g/l within the leaching fields in the early 1990s (Hradil and Hostomský, 1999).

Other usual sources of strong acidity in weathering crusts and soils are protons delivered from the oxidation either of NH_4^+ by bacteria (in soils) or Fe^{2+}. Precipitation of iron oxides in iron-rich environments (lateritic profiles in tropics), which releases large amounts of protons, can destabilize kaolinite in the crust (Ambrosi and Nahon, 1986). The same effect is given by the increased activity of organic acids coming either from organic matter decomposition or more directly from secretions of living organisms in soil (Robert and Tessier, 1992). We can conclude that extreme chemical action, low pH or very high water/rock ratios due to the heavy rainfall, produce oxide concentrations to the detriment of layered silicates (clays).

Kaolinite is the most common phase of the kaolinite group of layer-lattice minerals. The structural building block is the 'kaolinite layer', which can be regarded as a dioctahedral double layer, resulting from the joining of $(Si_4O_{10})^{4-}$ tetrahedral and $[(OH)_6Al_4(OH)_2]^{4+}$ octahedral (gibbsite) layers. Thus, the unit cell composition is $Al_4Si_4O_{10}(OH)_8$. Inner anion sites of kaolinite are occupied by both oxygen and hydroxyl groups. Outer anion sites are occupied by hydroxyl groups only and participate in reactions with protons at the solid/liquid interface (Wieland and Stumm, 1992). The structural disorder in kaolinite is given by sheet translation in the *b*-axis direction.

Several authors have studied dissolution kinetics of kaolinite under acidic conditions, such as Carroll-Webb and Walther (1988), Carroll and Walther (1990), Nagy et al. (1991), Wieland and Stumm (1992), Xie and Walther (1992), Ganor et al. (1995), Devidal et al. (1997) and Huertas et al. (1998). In all these studies, however, only pure mineral structures have been used. It should be evident that such laboratory data are not easily transferable to the behaviour of natural mineral associations—as (i) kaolinitic clays are very frequently accompanied by illitic material (illite is prevalent in temperate climatic zones) and other impurities in sediments and soils and (ii) the crystal structure of kaolinite is variable and ranges from triclinic to pseudomonoclinic forms; moreover (iii) the polymorphs (dickite, nacrite) can also occur. We have reported earlier (Hradil and Hostomský, 1999) that natural kaolinites taken from the sandstone matrix in the Stráž pod Ralskem uranium leaching area exhibit significant differences in their dissolution rates under the same experimental conditions.

The aim of the present work is to study the effect of mineral impurities and structural features upon the dissolution rate of different kaolinites under strong acid conditions, where the octahedral building layers are decomposed. We suppose that the kinetcs and mechanism of layered silicates dissolution are the crucial factors for the development of weathering profiles and the mobility of aluminium in acidified environment.

2. Materials and methods

Two samples of pure kaolinite with a significant difference in their crystallinity (KGa-1b and KGa-2, Georgia, USA), a commercial kaolin sample with 20 wt.% of illitic component (KIC-1, Sedlec, Czech Republic) and a sample of illitic clay with 20 wt.% of kaolinitic component (IMt-1, Montana, USA) were used in the kinetic experiments and the results compared with older data for KAO 6 and KAO 14 Cretaceous sandstone matrix kaolinites (Hradil and Hostomský, 1999).

Natural clay samples (KIC-1 and IMt-1) were dispersed in distilled water and the <2 μm fraction separated using the pipette method and Stokes Law (Borovec, 1992) to concentrate the clay minerals. X-ray powder diffraction was employed for mineralogical analyses using a SIEMENS D-5005 instrument under the following measurement conditions: CuKα radiation, secondary monochromator, voltage 40 kV, current 30 mA, degree range 2θ 3–90°, step 0.02° per 8 s. The raw data was processed by ZDS for Windows program (Ondruš, 1997) employing diffraction pattern database (JCPDS, 1999). Kaolinite, illite and quartz were identified in all samples; in the KGa-1b and KGa-2 samples traces of anatase were also found. In addition, normative mineral composition was calculated from the quantitative chemical analyses obtained by X-ray fluorescence. Vacuum X-ray spectrometer PHILIPS PW 1404/10 was used. Ideal formulae of the mineral phases are given by Deer et al. (1992) and Velde (1992); volatile compounds were excluded from the calculation of the normative composition.

Physical/chemical properties of KGa-1b and KGa-2 kaolinites are reported in Van Olphen and Fripiat (1979). Surface area of the KIC-1 and IMt-1 samples was determined by N_2 adsorption technique (BET; Brunauer et al., 1938) using Coulter SA3100 device. Physical parameters and mineral compositions are listed in Table 1, together with descriptions of KAO 6 and KAO 14 samples. These kaolinites were separated from sandstones of Cenomanian age in the area of uranium underground leaching (Stráž pod Ralskem, Czech Republic). Formation of KAO 6 kaolinite is related to later volcanic activity in the Tertiary, which caused alteration processes in nearby melilitic dykes. These authigenic kaolinites are usually accompanied by minerals of the crandallite group (aluminium phosphates). The origin of KAO 14 kaolinite is not known. It appears in the sandstones mostly as a fossil material weathered from the bedrock.

Structural disorder of kaolinite caused by the extent of the sheet translations is difficult to quantify. We express the structural disorder of kaolinite through the Hinckley index (I_H; Hinckley, 1963) and classify the samples as poorly crystallized with I_H<0.7 (KGa-2), partially ordered with I_H=0.7–1.0 (KIC-1, KAO 6) and well-ordered with I_H > 1.0 (KAO 14, KGa-1b) (Table 1). The Hinckley index is defined as the ratio of the sum of the heights of (1$\bar{1}$0) and (1$\bar{1}$1) diffraction peaks measured from their base and the height of (1$\bar{1}$0) peak measured from the background of the whole diffraction record. The problem of the characterisation of structural disorder is discussed in Artioli et al. (1995), Gaite et al. (1997) and Aparicio and Galan (1999).

In Hradil and Hostomský (1999), dissolution experiments with KAO 6 and KAO 14 kaolinites are described. Solutions of 0.05 M (pH=1.25) and 0.5 M (pH=0.65) sulphuric

Table 1
Mineral composition and physical properties of clay samples used in the kinetic experiments

	KGa-1b	KGa-2	KIC-1	IMt-1	KAO 6	KAO 14
Content of (wt.%)						
Kaolinite $Al_2Si_2O_5(OH)_4$	98	96	78	11	80	80
Illite $K_yAl_4(Si_{8-y}Al_y)O_{20}(OH)_4$, $y \approx 1.5$	traces	0.5	19	72	traces	2
Quartz SiO_2	–	–	2	9	2	3
Crandallite group $XAl_3H(OH)_6(PO4)_2$, X=Ca, Sr, Ba	–	–	–	–	7	3
Anatase TiO_2	2	2.5	<0.5	–	10	10
Hydrozircon $ZrSiO_4 \cdot nH2O$	–	–	–	–	–	2
Calcite $CaCO_3$	–	–	traces	1	<0.5	–
Goethite[a]	–	1	1	6	–	–
Pyrite[a]	–	–	–	1	–	–
BET surface area (m^2/g)	10.1	23.5	15.5	33.8	10.1	8.4
Grain size (μm)	<2	<2	<2	<2	<63	<63
Hinckley index for kaolinite (–)	1.38	0.23	0.91	–	1.00	1.13
References	Van Olphen and Fripiat (1979)				Hradil and Hostomský (1999)	

[a] Not found by X-ray diffraction; the contribution calculated from chemical analysis only.

acid were used at room temperature (22 and 23 °C, respectively). Calculated pH-dependent reaction rates are shown in Fig. 1. Both samples show very similar increases in weathering rate with decreasing pH, but the absolute values are different. The incongruence of the process expressed as the preferential removal of aluminium is significantly higher in the experiment with KAO 6 sample. To investigate the effects of composition and structural features on weathering rate, the following additional dissolution experiments were performed.

Leaching of the KGa-1b and KGa-2 samples suspended in 0.5 M H_2SO_4 solution (pH=0.65) at the 25 °C for 250 h to study the stoichiometry of the reaction, under saturated conditions with respect to amorphous SiO_2 precipitates (the limiting concentration of dissolved Si=0.002 mol/l at pH<9; Drever, 1988) and to quantify the influence of crystallinity upon the reaction rate. The solid/liquid ratio was 1:100 and the dissolution rate was calculated from the analytical measurements of Al and Si in the solution.

Leaching of KGa-1b, KIC-1 and IMt-1 samples suspended in 5 M H_2SO_4 solution at 40 °C for 48 h (accelerated experiments) to study the effect of the illitic impurities on the reaction rate. The solid/liquid ratio was 1:100 and the rate is calculated from the analytical measurements of Al in the solution. In these conditions, concentrations of dissolved Si have reached the limits given by precipitation of the amorphous SiO_2.

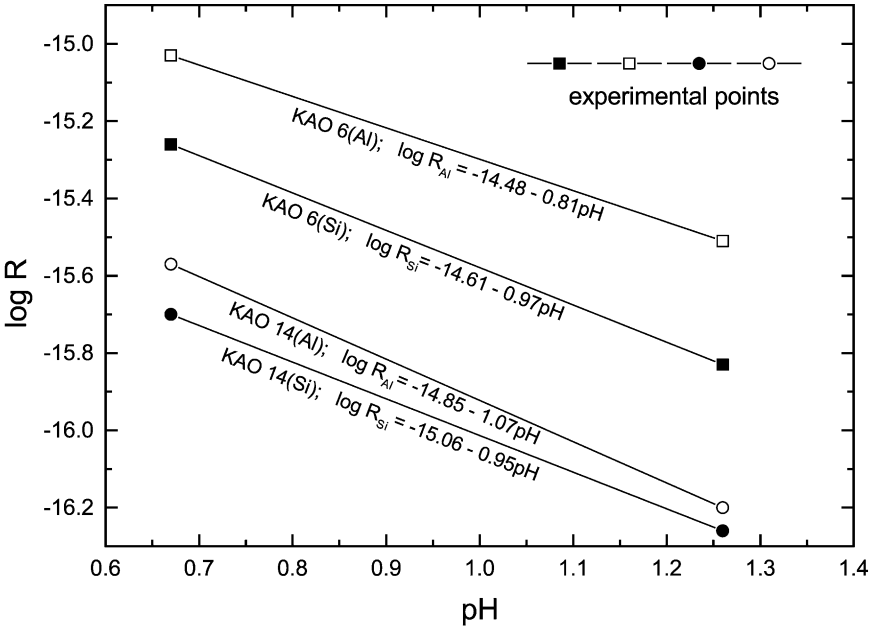

Fig. 1. Weathering rates of kaolinites in 0.05 and 0.5 M H_2SO_4, respectively, at room temperature as a function of pH. While the absolute dissolution rates of KAO 6 and KAO 14 kaolinites are different, their rise with decreasing pH is practically the same.

In each experiment, 100 ml polyethylene bottles were filled with 70 ml of the acid solution and the appropriate amount (0.7 g) of the solids was added. Then the bottles were placed into a thermostatic end-over-end shaker. In each defined time step, one bottle was taken off and the solid phase was separated in a centrifuge. Determination of the dissolved ions was performed using atomic absorption spectroscopy (Fe), emission spectrometry (K) (AAS-3 instrument, Carl Zeiss), gravimetry (Si) and spectrophotometry (Al and Si) (Spekol instrument, Carl Zeiss). Aluminium was determined using its complex with Chromazurol S after masking Fe by ascorbic acid (Malát, 1973). Monomeric and oligomeric silicic acid was determined as molybdosilicic acid (Malát, 1973).

3. Results and discussion

3.1. Stoichiometry of the process

In the early stages of the experiment, very fast non-stoichiometric dissolution was observed in all cases, with a preferential removal of aluminium. Then (usually after up to 50 h), a steady-state dissolution stage, with a linear increase of Si and Al concentrations was reached. Total amounts of released elements (in mols) were related to 1 cm^2 of the surface area of the solid sample, to eliminate differences in specific surface area, and then plotted against time. The steady-state parts of the experimental kinetic curves show good fits to linear regression lines and the reaction rates R (mol cm^{-2} s^{-1}) were derived from the slope of these lines. Results are listed in Table 2.

The Al/Si stoichiometry of the dissolution process of kaolinite in acidic solution is given by

$$\mathrm{Al_2Si_2O_5(OH)_4 + 6H^+ = 2Al^{3+} + 2H_4SiO_4 + H_2O}$$

When expressing the difference between the steady-state dissolution rates R (mol cm^{-2} s^{-1}) calculated from Al and Si concentrations, respectively, as $\Delta\log R=\log R_{\mathrm{Al}}-\log R_{\mathrm{Si}}$, a slight non-stoichiometry remains during the whole course of the dissolution of KGa-1b, KGa-2 and KAO 14 samples. In one case (KAO 6), a higher degree of non-stoichiometry was observed (Table 2, Fig. 2). The main reason for this is undoubtedly the increased amount of Al-rich impurities (phosphates of crandallite group) in the KAO 6 sample (Table 1).

Table 2
Reaction rates in 0.5 M solution of sulphuric acid

Sample	Duration (h)	T (°C)	R_{Si} (mol cm^{-2} s^{-1})	$\log R_{\mathrm{Si}}$	R_{Al} (mol cm^{-2} s^{-1})	$\log R_{\mathrm{Al}}$	$\log R_{\mathrm{Al}}-\log R_{\mathrm{Si}}$
KGa-1b	241	25	2.15×10^{-16}	−15.67	2.52×10^{-16}	−15.60	0.07
KGa-2	241	25	2.57×10^{-16}	−15.59	3.39×10^{-16}	−15.47	0.12
KAO 6	532	23	5.54×10^{-16}	−15.26	9.23×10^{-16}	−15.03	0.23
KAO 14	436	22	1.99×10^{-16}	−15.70	2.71×10^{-16}	−15.57	0.13

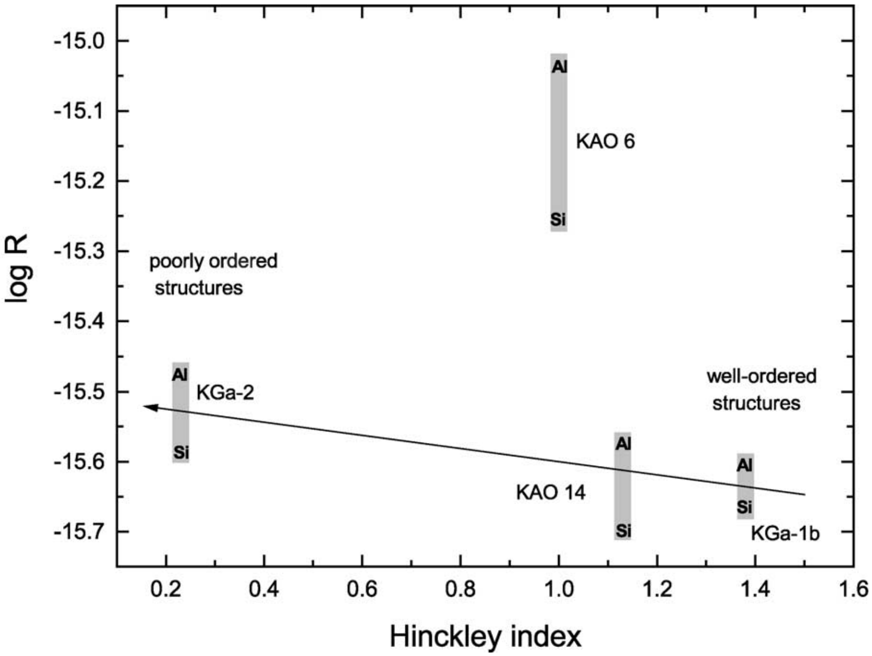

Fig. 2. Weathering rates (R in mol cm^{-2} s^{-1}) of kaolinites in 0.5 M H_2SO_4 and room temperature as a function of structural disorder (arrow). Non-stoichiometry is shown as the length of the bars where the top indicates the rate calculated from the Al concentrations and the bottom indicates the rate calculated from the Si concentrations in the solution, respectively.

3.2. *Effects of structural disorder*

The structural disorder of kaolinite given by sheet translation in the *b*-axis direction causes the 'opening' of the structure and thus an increase in specific surface area (compare the samples KGa-1b and KGa-2 in the Table 1). Since the reaction rates are related to a unit surface area, the effects of specific surface are eliminated and no other effects were initially expected. However, the weathering rate of poorly ordered KGa-2 kaolinite is higher if it is calculated from either Si or Al concentrations (Fig. 2). Both the so-called 'reference kaolinites' contain no significant impurities (Table 1); they were fractionated to the same grain size (<2 μm) and dissolved under the same conditions. We suppose that (i) only structural features can cause the observed differences in the rates and (ii) the disordered open structures are more easily accessible for proton attack at the edges and at the basal surfaces with outer hydroxyls groups. On the other hand, the effect of structural disorders described above is too small to explain the behaviour of natural samples (KAO 6 and KAO 14). These samples represent partially or well-ordered kaolinites. Their crystal structure is not as perfect as that of the KGa-1b kaolinite; and this is apparent from the lower values of the Hinckley index (Fig. 2). The unusual behaviour of KAO 6 kaolinite cannot, however, be fully explained by the effect of

Table 3
Reaction rates in 5 M solution of sulphuric acid

Sample	Duration (h)	T (°C)	R_{Al} (mol cm^{-2} s^{-1})	logR_{Al}	R_K (mol cm^{-2} s^{-1})	logR_K
KGa-1b	46.5	40	7.28×10^{-15}	−14.14		
KIC-1	46.5	40	4.95×10^{-15}	−14.30		
IMt-1	45.5	40	2.48×10^{-15}	−14.61	1.49×10^{-16}	−15.83

structural disorder; one explanation could be that the increased content of crandallites also affects the structure of kaolinite.

3.3. Effects of illitic admixtures

In sediments, soils and weathering crusts, illites commonly accompany kaolinites and as additional sources of aluminium and silicon they could affect weathering rates in acidic conditions. They are chemically variable and thus their content is difficult to calculate from chemical analyses. Using the averaged crystallochemical formula of Velde (1992), we selected three samples: one with no illitic material (KGa-1b) and the others with significant (KIC-1) and major (IMt-1) amounts of illite (see Table 1). Dissolution was accelerated by increasing the acid concentration (5 M H_2SO_4) and the temperature (40 °C), thus the steady-state stage of the process was reached after about 10 h of reaction. Dissolution rates were calculated from the concentration of aluminium (Table 3); the course of dissolution is shown in Fig. 3. When comparing results it is evident that with increasing illite content, the dissolution rates of the clay samples decrease.

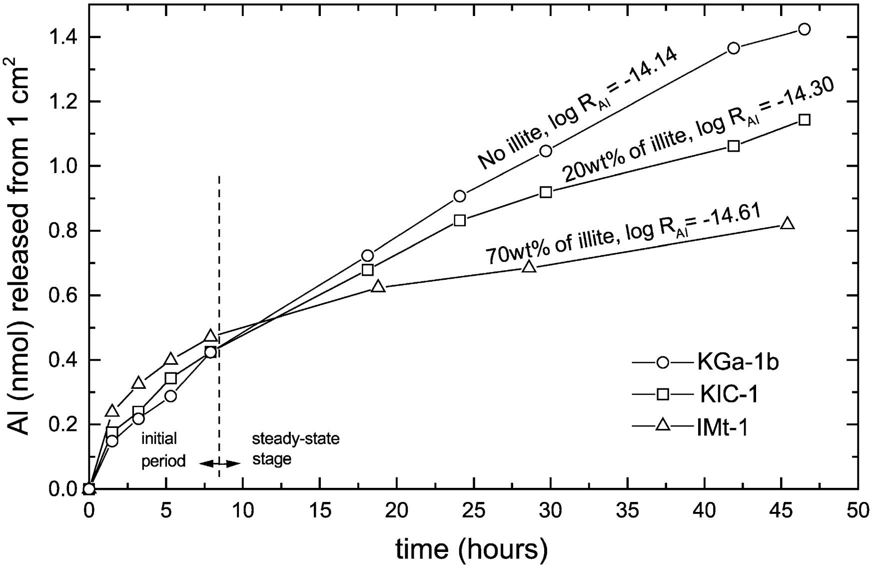

Fig. 3. Weathering rates (R in mol cm^{-2} s^{-1}) of kaolinites in 5 M H_2SO_4 and 40 °C as a function of illitic admixtures. Calculated from Al concentrations.

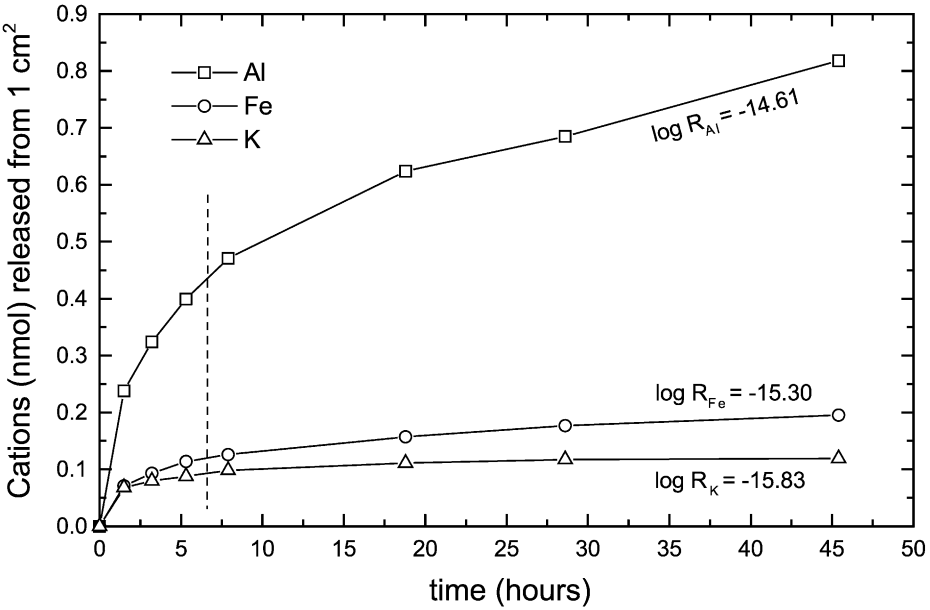

Fig. 4. Weathering rate (R in mol cm^{-2} s^{-1}) of the IMt-1 sample in 5 M H_2SO_4 and 40 °C calculated from the release of different elements. In the steady-state stage of dissolution, aluminium is released from kaolinite and illite, iron possibly partly from iron hydrooxides and partly from clay minerals, potassium from illite only.

In the case of the IMt-1 sample with dominant illite (72 wt.%), higher amounts of K and Fe are also released. If we compare the concentrations of these elements we see great differences in the slopes of their growth over a period of time. The increase of concentration of aluminium is fast, because it is supported by both kaolinite and illite. Iron is released either from free hydrooxides and/or from kaolinite and illite, where it can substitute for aluminium in octahedral positions. Potassium is released only from illite and thus the increase of its concentration is the slowest (Fig. 4). The results indicate that the acid-weathering rate of pure illite is very slow compared with that of kaolinite.

4. Conclusions

We have found that the acid weathering rate of kaolinitic clays is strongly influenced by their nature. For example, dissolution of sample KAO 14 at pH=0.65 is as fast as the dissolution of KAO 6 at pH=1.25 (see Fig. 1). Weathering rates increase with structural disorder of kaolinite, but observed differences cannot be fully explained by the diversity of crystal lattice structures.

Mineral impurities that appear commonly in natural kaolinites can affect the weathering rate and also the Al/Si stoichiometry of the process (as shown by aluminium phosphates–crandallites-accompanying clay minerals in altered rocks at the contact with melilitic dykes).

The presence of illites undoubtedly slows down the acid decomposition of clays. As was shown in the experiments with concentrated acid solutions, the dissolution rate decreases with increasing illite content in the mixture with kaolinite; the contribution of illite itself to the dissolution process is very small.

Finally, the contribution and position of octahedral (aluminium bearing) sites (which is different in 1:1 and 2:1 clay structures), ordering of structural layers of clay minerals and the presence of non-clay impurities can all significantly affect the rate of acid decomposition of kaolinite-rich materials and therefore the subsequent release and mobility of aluminium and silicon. When calculating solute transport in acidified profiles it is therefore suggested that changes in the kinetic parameters of kaolinite due to the presence of poorly ordered structures (increasing the rate) and to the presence of 2:1 structures (such as illites, decreasing the rate) in mineral assemblages should be taken into account. Such a correction should be incorporated when modelling future development of any weathering profile, but the significance of differences described above increases when dissolution of kaolinite is accelerated by strong acid inputs (polluted areas) and/or by elevated temperatures (hydrothermal alteration).

Acknowledgements

This work was supported by the Grant Agency of the Czech Republic (Grant No. 203/98/P203). The authors are very grateful to their colleagues from the Institute of Inorganic Chemistry, Academy of Sciences of the Czech Republic (Petr Bezdička and Antonín Petřina—X-ray diffraction, Tomáš Grygar—spectroscopic and spectrophotometric methods, Václav Štengl—BET surface measurements) and from the Gematest Prague, (Alexander Manda—X-ray fluorescence) for performing the measurements and for their help with the interpretations of the results.

References

Ambrosi, J.P., Nahon, D., 1986. Petrological and geochemical differentiation of lateritic iron crust profiles. Chem. Geol. 57, 371–393.

Aparicio, P., Galan, E., 1999. Mineralogical interference on kaolinite crystallinity index measurements. Clays Clay Miner. 47 (1), 12–27.

Artioli, G., Bellotto, M., Gualtieri, A., Pavese, A., 1995. Nature of structural disorder in natural kaolinites: a new model based on computer simulation of powder diffraction data and electrostatic energy calculation. Clays Clay Miner. 43 (4), 438–445.

Borovec, Z., 1992. Laboratorní Metody Výzkumu Hornin a Minerálů. Charles University, Prague (in Czech).

Brunauer, S., Emmet, P.H., Teller, E., 1938. Adsorption of gases in multimolecular layers. J. Am. Chem. Soc. 60, 309–319.

Carroll, S.A., Walther, J.V., 1990. Kaolinite dissolution at 25, 60 and 80 °C. Am. J. Sci. 290, 797–810.

Carroll-Webb, S.A., Walther, J.V., 1988. A surface complex reaction model for the pH-dependence of corundum and kaolinite dissolutions rates. Geochim. Cosmochim. Acta 52, 2609–2623.

Deer, W.A., Howie, R.A., Zussman, J., 1992. An Introduction to the Rock-Forming Minerals Longman, New York.

Devidal, J.L., Schott, J., Dandurand, J.L., 1997. An experimental study of kaolinite dissolution and precipitation kinetics as a function of chemical affinity and solution composition at 150 °C, 40 bars, and pH 2, 6.8, and 7.8. Geochim. Cosmochim. Acta 61, 5165–5186.

Drever, J.I., 1988. The Geochemistry of Natural Waters Prentice-Hall, Englewood Cliffs, NJ.

Gaite, J.M., Ermakoff, P., Allard, T., Muller, J.P., 1997. Paramagnetic Fe^{3+}: a sensitive probe for disorder in kaolinite. Clays Clay Miner. 45 (4), 496–505.

Ganor, J., Mogollón, J.L., Lasaga, A.C., 1995. The effect of pH on kaolinite dissolution rates and on activation energy. Geochim. Cosmochim. Acta 59, 1037–1052.

Hinckley, D.N., 1963. Variability in crystallinity values among kaolin deposits of the coast plain of Georgia and South Carolina. Clays Clay Miner. 11, 229–235.

Hradil, D., Hostomský, J., 1999. Dissolution kinetics of natural kaolinites at low pH sulfuric acid solutions— an example from Stráž pod Ralskem mineral deposit. Acta Univ. Carol., Geol. 43 (3), 537–543.

Huertas, F.J., Chou, L., Wollast, R., 1998. Mechanism of kaolinite dissolution at room temperature and pressure: Part 1. Surface speciation. Geochim. Cosmochim. Acta 62, 417–431.

JCPDS, Powder Diffraction File, PDF-2 Sets 1–49, 1999. International Centre for Diffraction Data, Newtown, PA.

Malát, M., 1973. Absorpční Anorganická Fotometrie. Academia, Prague, Czech Republic (in Czech).

Milnes, A.R., Thiry, M., 1992. Silcretes. In: Martini, I.P., Chesworth, W. (Eds.), Weathering, Soils and Paleosols. Elsevier, Amsterdam, pp. 349–377.

Nagy, K.L., Blum, A.E., Lasaga, A.C., 1991. Dissolution and precipitation kinetics of kaolinite at 80 °C and pH 3. The dependence on solution saturation state. Am. J. Sci. 291, 649–686.

Ondrus, P., 1997. ZDS—Software for X-ray Powder Diffraction Analysis ZDS Systems, Prague, Czech Republic.

Robert, M., Tessier, D., 1992. Incipient weathering: some new concepts on weathering, clay formation and organization. In: Martini, I.P., Chesworth, W. (Eds.), Weathering, Soils and Paleosols. Elsevier, Amsterdam, pp. 71–105.

Sucha, V., Kraus, I., Stresko, V., Samajová, E., 1994. Aluminium pollution due to the pyrophyllite dissolution by sulphuric acid near Banská Stiavnica, Slovakia. In: Melka, K. (Ed.), Book of Abstracts of the XIIIth Conference on Clay Mineralogy and Petrology. Prague, Czech Republic, August 29–September 2, 1994, p. 108.

Thiry, M., Simon-Coinçon, R., 1996. Tertiary paleoweatherings and silcretes in the southern Paris basin. Catena 26 (1–2), 1–26.

Thiry, M., Bertrand Ayrault, M., Grisoni, J.C., 1988. Ground-water silicification and leaching in sands: example of the Fontainebleau Sand (Oligocene) in the Paris basin. Geol. Soc. Am. Bull. 100, 1283–1290.

Van Olphen, H., Fripiat, J.J., 1979. Data Handbook for Clay Minerals and Other Non-Metallic Materials. Pergamon, London.

Velde, B., 1992. Introduction to Clay Minerals. Chapman & Hall, London.

Wieland, E., Stumm, W., 1992. Dissolution kinetics of kaolinite in acidic solutions at 25 °C. Geochim. Cosmochim. Acta 56, 3339–3355.

Xie, Z., Walther, J.V., 1992. Incongruent dissolution and surface area of kaolinite. Geochim. Cosmochim. Acta 56, 3357–3363.